Efficient Single-Jet Mixing in Turbulent Tube Flow

L. J. FORNEY
and
T. C. KWON
Department of Civil Engineering
University of Illinois
Urbana, Illinois 61801

A similarity law is proposed to provide effective jet penetration and mixing of a tracer in turbulent tube flow. The scaling law is derived from approximate solutions to the equations of motion for the case of a single, fully developed turbulent jet issuing normally to the flow. Jet properties are correlated with experimental measurements on a methane tracer.

SCOPE

Circumstances frequently require effective mixing of two fluids in the chemical industry. Good mixing is often necessary, for example, to obtain profitable yields or to eliminate excessive corrosion in reactor or combustion chambers. Although the continuous mixing of two fluid streams can be achieved using a number of techniques, many procedures such as the use of baffles will introduce an excessive pressure drop. An effective simple method is to introduce a fluid into a tube cross flow or mainstream with a single turbulent jet such that jet contact with tube walls is minimized and mixing occurs rapidly within the tube core.

Chilton and Genereaux (1930) injected smoke jets into crossing air streams flowing in large glass tubes and studied the resultant mixing visually. They concluded that right-angle configurations were as effective as any other for good mixing. Since the pioneering effort of Chilton and Genereaux, several investigators have studied the intermixing of turbulent jets in confined cross flows. Recently, Ger and Holley (1974) measured the concentration of a sodium chloride tracer at large distances (~100 duct diameters) from the jet orifice and recorded the momentum flux ratios for conditions which minimized the distance required for complete mixing. All of these works have acknowledged the importance of understanding near field properties, but a correlation of reliable data with a theory based on a criterion for effective mixing is currently lacking.

The objective of this study is to provide reliable data on jet properties within several tube diameters from the jet orifice, to develop a simple criterion judged to constitute a condition of effective penetration and unretarded mixing, and to correlate the data with theoretical predictions.

CONCLUSIONS AND SIGNIFICANCE

A scaling law is derived for a single, fully developed turbulent jet issuing normally into a tube cross flow where it is assumed that for some distance from the orifice, defined as the near field, effects of ambient turbulence on the mixing process can be neglected relative to jet induced turbulence. Boundary conditions imposed on approximate solutions to the equations of motion provide geometrically similar jet trajectories centering the jet and tube axes in the near field to minimize jet contact with tube walls, and this condition is used as a criterion for effective penetration and unretarded mixing. Experiments were performed with a methane jet of large Reynolds number whose properties (position and relative concentrations) were determined with a flame ionization detector. The theory is shown to adequately correlate the data and selected data of others to within 35%. The results indicate that for both large jet Reynolds number $Re_j > 0.9 \times 10^4$ and Froude number, effective mixing can be achieved by properly choosing the ratio of jet to tube velocity $R = u_o/v$ for a given jet to tube diameter d/D.

The problem of mixing two fluids by a turbulent jet issuing normally into a confined turbulent cross flow has numerous important applications as suggested by a number of researchers. For example, Hoult and Weil (1972) comment on the use of cool gas jets directed normally to the flow of hot gases as a means of controlling the heat transfer rate to ducts. Likewise, Ger and Holly (1974) suggest the application of jets to controlled pipe mixing in order to chlorinate water supplies or neutralize harmful waste material with chemical additives in industrial effluents, in addition to the simple use of tracers for discharge measurements within pipes. Moreover, Stoy and Ben-Haim (1973) point out the importance of jets in cooling schemes for turbine blades and in the technology of certain kinds of low flying aircraft. Finally, Chilton and Genereaux (1930) suggest the use of turbulent jets for the mixing of fuels prior to combustion chambers and gas Bunsen burners. In all of these applications, it is desirable to achieve effective mixing of both fluids in a short distance from the jet orifice.

L. J. Forney is presently at the School of Chemical and Civil Engineering, Georgia Institute of Technology, Atlanta, Georgia 30332.

0065-8812-79-2718-0623-$01.05.

The understanding of turbulent jets and plumes in a cross flow has progressed rapidly in the past two decades (for the highlights of this development, see Hoult and Weil, 1972). Theoretical descriptions of these flows have been based on simple dimensional arguments (for example, Scorer, 1958), entrainment models (for example, Hoult, Fay, and Forney, 1969), and eddy viscosity or mixing length assumptions (for example, Slawson and Csanady, 1967). Numerous laboratory experiments on jets and plumes in a cross flow have been conducted with both air and water as working fluids (for example, Keffer and Baines, 1963). Most of the work, however, has been directed at understanding either the basic nature of the flow, such as that of Keffer and Baines (1963), or applying the results to buoyant plumes in the atmosphere, as outlined in a review by Briggs (1969). Little attention has been given specifically to mixing processes in confined cross flows where the velocity profile typically resembles that of turbulent tube flow.

The first attempt to study the process of jet mixing in tube flows was that of Chilton and Genereaux (1930). Although no attempt was made to predict the theoretical behavior of jets in a pipe, they were able to quantitatively identify what constituted good mixing by visually observing the character of a thick smoke tracer within glass tubes. Recently, however, additional experimental and theoretical work on the mechanics of jets in confined cross flows has been conducted by Mozharov, Chikelevskaya, and Kormilitsyn (1972), Stoy and Ben-Haim (1973), and Ger and Holley (1974), while only the latter work was concerned with the effectiveness of the mixing process.

A limitation to much of the theoretical work done with jets and plumes is the assumption of laminar cross flows while most, in practice, are turbulent. Turbulent cross flows exist not only within the atmospheric boundary layer (Briggs, 1969) but also commonly in tubes which have a Reynolds number in the range of $10^4 < Re < 10^6$ (Ger and Holley, 1974). Hence, the usual approach to practical problems has been to divide the mixing process into two regions: a near field in which the mixing is dominated by jet induced turbulence and a far field where ambient turbulence predominates.

This paper uses a simple entrainment model to derive a scaling law close to the jet orifice for the case of a single jet directed normally into turbulent tube flow. The scaling law is derived by assuming that effective penetration and mixing occurs, a condition in which the jet is not retarded by the tube walls, when the jet is geometrically centered along the tube axis at a fixed distance from the orifice. The expression is used to correlate published data including recent experimental results.

THEORY

The phenomenon of jet mixing of a tracer in turbulent tube flow involves two phases. In the initial stage, the mixing process is dominated by self-induced jet turbulence. After a distance (or time) defined as the near field for a geometrically centered jet, that is, one that does not impinge on the large tube wall as seen in Figure 1, it is presumed that the injected fluid sufficiently equilibrates with the ambient turbulent flow. Beyond the near field, mixing of the tracer is dominated by turbulence in the main stream. [For similar arguments describing the mixing of jets and plumes in the atmosphere see Briggs (1969).] With this hypothesis it is assumed that one can insure effective penetration or unretarded mixing conditions by describing the trajectory of the jet in the near field. This presumably would insure effective mixing within a few duct diameters from the jet entrance and

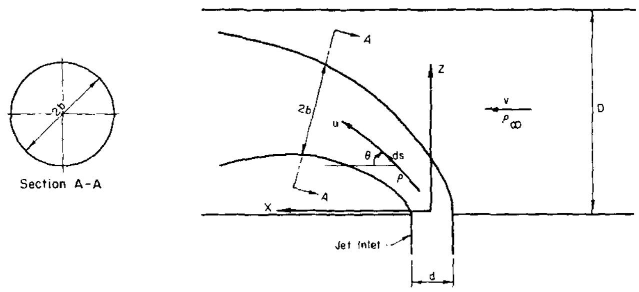

Fig. 1. Coordinate system for a jet in a tube cross flow.

minimize the distance far down the tube axis required to achieve complete mixing.

There are four characteristic lengths in the problem which determine the scale of the jet trajectory within the tube. These length scales are the jet nozzle diameter $d = 2b_o$ (see Figure 1), the tube diameter D, a length l_m representing the distance over which the jet travels before it bends over in the cross flow, and, finally, the length of the near field l_D over which the ambient turbulence can be neglected in the mixing process. For a jet issuing normally into the cross flow and neglecting the effects of buoyancy, one can define a momentum length scale l_m by

$$l_m \equiv \frac{du_o}{v} \tag{1}$$

which represents the distance over which the normal momentum flux of entrained fluid is comparable to its initial value at the orifice. Moreover, if v/ω represents the ratio of mean cross flow velocity v to an angular frequency ω, where $\omega \simeq \pi(u^*/l)$, a distance is defined sufficiently close to the orifice over which the effects of ambient turbulence can be neglected. The near field length scale l_D is then defined as

$$l_D \equiv \frac{v}{\omega} \tag{2}$$

which physically represents the distance a parcel of fluid travels down the duct axis before it diffuses laterally over a distance comparable to the Prandtl eddy mixing length. The importance of this length in turbulent tube flow was illustrated by Kalinske and Pien (1944).

In order to efficiently correlate experimental data, it is convenient to form three dimensionless groups from the four lengths described above. The first is defined as the velocity ratio R equal to the ratio of the momentum length to the orifice diameter:

$$R = \frac{u_o}{v} = \frac{l_m}{d} \tag{3}$$

The second represents the ratio of the near field length to duct diameter l_D/D, while the third is the ratio of the momentum length to duct diameter l_m/D.

The entrainment model used in this paper is based on the M.I.T. theory developed by Hoult, Fay, and Forney (1969) to explain the rise and growth of turbulent plumes in laminar cross flows. A discussion of the theory and assumptions and its application to a number of laboratory and field conditions are given in a number of other works (for example, Hoult, Fay, and Forney, 1969; Hoult and Weil, 1972; Fay, 1973). Here, the approach to the problem is to derive approximate expressions for the jet properties in the near field, where $x/l_D \leq 1$ for a jet issuing perpendicularly into the cross flow. Thus, assuming a uniform (top hat) velocity profile in the jet for the geometry of Figure 1 with boundary conditions at the orifice $s = 0$ of $u = u_o$, $b = b_o$, $c = c_o$ and $\theta_o = \pi/2$, one has for small departures from θ_o ($\theta \simeq \pi/2$) the conservation of mass

$$\frac{d}{ds}(\pi b^2 u) = 2\pi b_o(\alpha u_o + \beta v) \quad (4)$$

tangential momentum

$$\frac{d}{ds}(u^2 \pi b^2) = 0 \quad (5)$$

normal momentum

$$u_o^2 \pi b_o^2 \frac{d\theta}{ds} = -v\frac{d}{ds}(\pi b^2 u) \quad (6)$$

and tracer concentration

$$\frac{d}{ds}(c\pi b^2 u) = 0 \quad (7)$$

Furthermore, the orifice Reynolds number ($Re_j = u_o d/\nu$) is restricted to large values to insure jet turbulence, while the effect of buoyancy is neglected or $\rho \simeq \rho_\infty$ (see Appendix). Solution of the approximate expressions Equations (4) to (6) gives to first order

$$\frac{b^2 u}{b_o^2 u_o} = 1 + 4(\alpha + \beta/R)s/d \quad (8)$$

$$u^2 b^2 = u_o^2 b_o^2 \quad (9)$$

$$\theta = \pi/2 - 4\left(\alpha + \frac{\beta}{R}\right)\left(\frac{s}{l_m}\right) \quad (10)$$

while integrating Equation (7) and rearranging, we get

$$\frac{c}{c_o} = \frac{1}{1 + 4(\alpha + \beta/R)s/d} \quad (11)$$

Finally, since $dz \simeq ds$ and $dx \simeq (\pi/2 - \theta)ds$ near the jet orifice, one can write an approximate expression for the jet trajectory as

$$\frac{z}{l_m} = \left[\frac{1/2}{\alpha + \frac{\beta}{R}}\right]^{1/2}\left(\frac{x}{l_m}\right)^{1/2} \quad \text{for} \quad \frac{x}{l_m} < 1 \quad (12)$$

At this point, it is useful to discuss the restriction $x/l_m < 1$ on Equation (12). In order to center the jet in the tube, one assumes that the momentum length of the jet is greater than the combined thickness of the laminar and buffer regions of the turbulent shear layer but less than the duct diameter, or roughly that $0.1 < (l_m/D) < 0.9$. Furthermore, for a parcel of injected fluid, the normalized position at time ω^{-1} is

$$\frac{x}{D} \simeq \frac{l_D}{D} \quad (13)$$

where the assumption in Equation (13) is tentatively made that a fluid parcel within the jet has traveled sufficiently far from the orifice so that $x \simeq v/\omega$ (see Appendix). One can now substitute Equation (2) into Equation (13), where $l = 0.08D$, $u^* = \phi^{1/2}v$, $\phi^{1/2} = 0.2\ Re^{-1/8}$, and 2ϕ is the Fanning friction factor (Davies, 1972). This demonstrates that over a wide range of tube Reynolds numbers $10^4 < Re < 10^6$, the length of the normalized near field is $l_D/D \simeq 0.4/\pi\ Re^{1/8} \simeq 0.5$ or is approximately a constant. A complete analysis of the approximate solutions to Equations (4) to (6) is given in Hoult and Weil (1972). They indicate that the range of validity of Equation (12) formally depends on the velocity ratio R of the flow and that numerical solutions to Equations (4) to (6) do not significantly deviate from the approximate result until $x >> l_m$. These arguments support use of Equation (12) in the near field for $x < l_D$.

To insure effective mixing in the duct, one now seeks all geometrically similar jet trajectories where the jet center line is centrally located at $x \simeq l_D \simeq 0.5\ D$. Normalizing the jet coordinates in Equation (12) with respect to the duct diameter D, one has

$$\frac{z}{D} = \left[\frac{1/2}{\alpha + \frac{\beta}{R}}\right]^{1/2}\left(\frac{l_m}{D}\right)^{1/2}\left(\frac{x}{D}\right)^{1/2} \quad (14)$$

where the boundary conditions for a centered jet are $z/D = x/D = 0.5$. This yields the simple criterion

$$\frac{l_m}{D} = \alpha + \frac{\beta}{R} \quad \text{for} \quad R > 1 \quad (15)$$

where the entrainment parameters are universal constants with assumed values of $\alpha = 0.11$ and $\beta = 0.6$ (see Hoult and Weil, 1972). Implicit in the derivation of Equation (15) is the assumption that $b/D < 1$ or that wall effects are unimportant. If one assumes that $b_o/D << 1$ or that $R > 1.0$, then the neglect of the potential core in the analysis is justified since its length in a turbulent jet is scaled by the orifice diameter (for example, Stoy and Ben-Haim, 1973).

It follows from Equations (8), (9), (11), and (15) that the near field properties for geometrically centered jets such as the mean tracer concentration and jet velocity are

$$c/c_o = u/u_o = \frac{1}{1 + 2^{3/2}R\left(\frac{x}{D}\right)^{1/2}} \quad (16)$$

where the mean jet radius is

$$\frac{b}{b_o} = 1 + 2^{3/2}R\left(\frac{x}{D}\right)^{1/2} \quad (17)$$

In addition to predicting jet properties, a useful design requirement for these flows is the mixing ratio or volume rate of tracer to tube flow as a function of the velocity ratio R. From Equation (15), the mixing ratio for a given $R > 1$ can be expressed as

$$\frac{d^2 u_o}{D^2 v} = \left(\frac{l_m}{D}\right)^2\left(\frac{1}{R}\right) = \left(\alpha + \frac{\beta}{R}\right)^2 \frac{1}{R} \quad (18)$$

Using Equation (18), one can determine the necessary velocity ratio R for a specified mixing ratio. The required

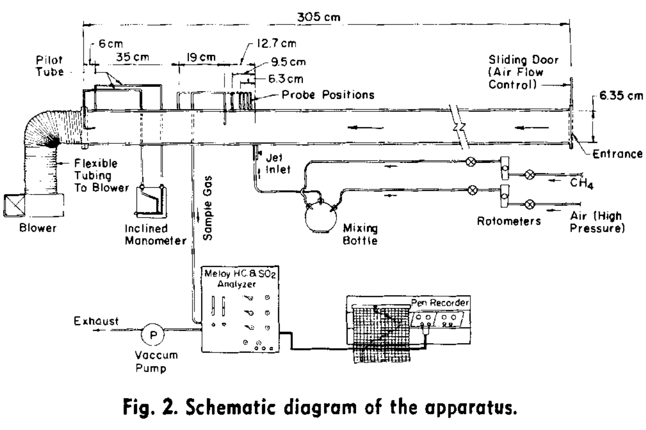

Fig. 2. Schematic diagram of the apparatus.

Table 1. Summary of Experimental Data*

	d (cm)	d/D	u_o (cm/s)	v (cm/s)	R ($= u_o/v$)	Avg	l_m/D	Avg	Re ($\times 10^4$)	Re_j ($\times 10^4$)
					$x/D = 2.0$					
Max	1.27	0.2	1 180	447	2.48	2.44	0.50	0.49	2.50	0.99
Min	1.27	0.2	2 422	990	2.45		0.49		5.12	2.05
Max	0.95	0.15	4 084	1 465	2.79	2.73	0.42	0.42	7.50	2.59
Min	0.95	0.15	1 877	679	2.76		0.42		3.54	1.19
Max	0.64	0.10	5 464	1 465	3.73	3.59	0.37	0.36	7.50	2.31
Min	0.64	0.10	2 360	679	3.47		0.35		3.54	0.99
Max	0.48	0.076	7 075	1 465	4.83	4.42	0.37	0.33	7.50	2.25
Min	0.48	0.076	4 201	1 085	3.87		0.30		5.59	1.33
Max	0.32	0.05	4 769	1 085	4.39	4.34	0.22	0.22	5.59	1.01
Min	0.32	0.05	6 358	1 465	4.34		0.22		7.50	1.35
Max	0.24	0.038	7 424	1 465	5.07	4.96	0.19	0.19	7.50	1.18
Min	0.24	0.038	6 364	1 289	4.94		0.19		6.62	1.01
Max	0.16	0.025	10 332	1 465	7.05	6.98	0.18	0.18	7.50	1.09
Min	0.16	0.025	9 538	1 379	6.91		0.17		7.07	1.01
					$x/D = 3.0$					
Max	1.27	0.2	1 890	720	2.62	2.56	0.52	0.51	3.80	1.61
Min	1.27	0.2	1 303	520	2.50		0.50		2.70	1.10
Max	0.95	0.15	2 318	836	2.77	2.73	0.42	0.41	4.33	1.47
Min	0.95	0.15	3 201	1 191	2.69		0.40		6.10	2.03
Max	0.64	0.10	2 608	836	3.12	3.10	0.31	0.30	4.33	1.10
Min	0.64	0.10	3 974	1 288	3.08		0.30		6.62	1.68
Max	0.48	0.076	5 749	1 379	4.3	3.96	0.326	0.30	7.07	1.83
Min	0.48	0.076	3 740	1 626	3.64		0.276		5.31	1.17
Max	0.32	0.05	7 948	1 697	4.69	4.50	0.234	0.23	8.66	1.67
Min	0.32	0.05	5 166	1 191	4.34		0.217		6.13	1.09
Max	0.24	0.038	8 850	1 697	5.2	4.91	0.198	0.19	8.66	1.40
Min	0.24	0.038	6 363	1 379	4.62		0.175		7.07	1.01
Max	0.16	0.025	11 125	1 767	6.32	6.24	0.158	0.16	9.02	1.18
Min	0.16	0.025	9 538	1 546	6.16		0.154		7.91	1.01
					$x/D = 5.0$					
Max	1.27	0.02	2 484	1 085	2.29	2.30	0.46	0.46	5.59	2.10
Min	1.27	0.02	1 552	679	2.28		0.46		3.54	1.31
Max	0.95	0.15	3 864	1 465	2.64	2.56	0.40	0.38	7.50	2.45
Min	0.95	0.15	1 711	679	2.52		0.38		3.54	1.09
Max	0.64	0.10	4 471	1 465	3.05	2.97	0.31	0.31	7.50	1.89
Min	0.64	0.10	2 484	836	2.97		0.30		4.33	1.05
Max	0.48	0.076	5 749	1 465	3.92	3.57	0.3	0.27	7.50	1.83
Min	0.48	0.076	3 759	1 085	3.46		0.26		5.59	1.19
Max	0.32	0.05	4 769	1 289	3.70	3.61	0.18	0.18	6.62	1.01
Min	0.32	0.05	5 166	1 465	3.53		0.18		7.50	1.09
Max	0.24	0.038	7 950	1 733	4.58	4.43	0.174	0.17	8.8	1.21
Min	0.24	0.038	6 420	1 505	4.27		0.165		7.7	1.02
Max	0.16	0.025	—	—	—	6.20	—	0.155	—	—
Min	0.16	0.025	10 900	1 767	6.20		0.155		9.0	1.07

* Tube diameter $D = 6.35$ cm, $\nu = 0.15$ cm²/s.

ratio of jet to tube diameter d/D can then be determined from Equation (15).

EXPERIMENTAL METHODS

The experimental technique consisted of measuring the center line position and concentration of a fully turbulent methane jet issuing normally into a turbulent air stream flowing through a 6.35 cm lucite I.D. tube. The primary airflow was maintained with a blower located downstream from the jet orifice and measured with a pilot tube as shown in the schematic of the apparatus in Figure 2. The air velocity within the larger tube was regulated by restricting the cross-sectional area of the entrance which increased the head loss and lowered the flow rate. It was found that tube Reynolds numbers of up to $Re = 6.3 \times 10^4$ could be obtained in this manner.

The mean jet orifice velocity u_o was measured with a calibrated rotameters as indicated in Figure 2 and regulated with a high pressure gauge. The jet diameter was varied in the experiment by using one of seven lucite inserts covering the range $0.16\text{ cm} < d < 1.27\text{ cm}$ as indicated in Table 1. The jet air flow was regulated with a high pressure gauge up to $Re_j = 2.4 \times 10^4$ which was sufficient to center the jet axis and to insure fully developed turbulence within the jet.

Jet concentration profiles were determined with one of several probes which were adjustable along the tube radii and were located at a number of positions downstream from the jet orifice. Methane concentrations were measured along the tube diameter with a flame ionization detector (Meloy) and continuously recorded with a pen recorder. The methane was premixed with air in a 1 l beaker, and the total jet flow rate was measured by the rotameters shown in Figure 2.

The procedure for a typical run with a fixed jet to tube diameter d/D was to establish the air flow in the large tube at one of several values of the Reynolds number covering the range $2.5 \times 10^4 < Re < 7.5 \times 10^4$. Concentration profiles were varied and determined at each value of Re for probe positions $x/D = 2.0$, 3.0, and 5.0 while increasing the jet

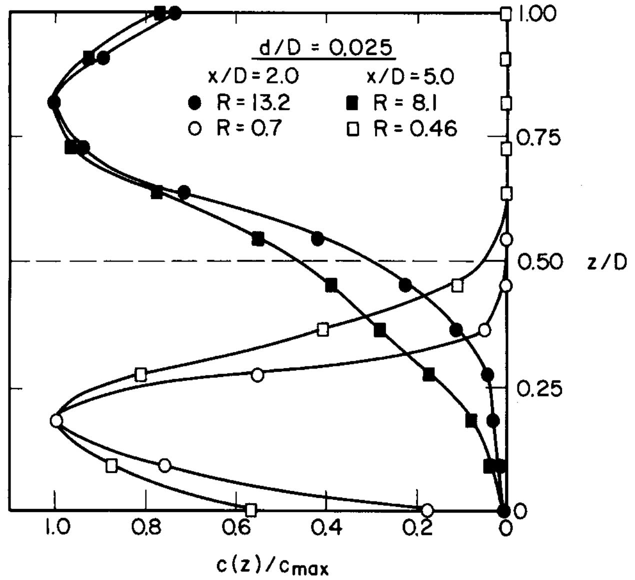

Fig. 3. Methane concentration profiles for cases of poor mixing. Solid symbols correspond to overpenetration, while open symbols indicate underpenetration.

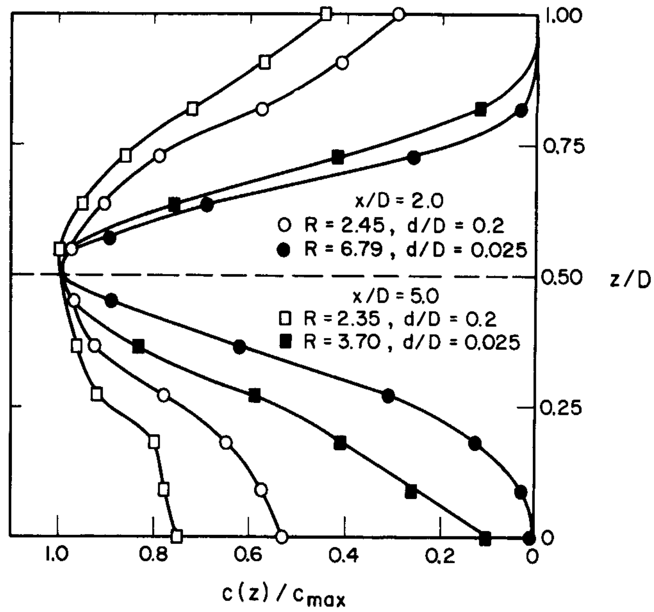

Fig. 4. Methane concentration profiles for geometrically centered jets.

velocity until the center line of the methane jet coincided with the tube center line. The maximum and minimum values of the velocity ratio ($R = u_o/v$) for geometrically centered jets at each jet to tube diameter d/D for the indicated range of Re are shown in Table 1. Several values of R and l_m/D over the indicated range were used to compute the listed averages. Methane jet center-line concentrations were also recorded at several additional probe locations downstream from the jet orifice for several jets previously centered at $x/D = 2.0$.

RESULTS AND DISCUSSION

Table 1 summarizes the experimental data judged to constitute a condition of effective penetration or mixing for geometrically centered jets covering a range in velocity ratios of $2.3 < R < 7.05$. For a given jet to tube diameter, only a small range of velocity ratios R appeared to provide a geometrically centered jet. If the velocity ratio R was too small, the methane tracer remained along the tube wall and failed to sufficiently penetrate the cross flow. Conversely, if R was too large, the jet overpenetrated the tube center line and subsequently impacted with the opposite wall. These latter conditions are illustrated in Figure 3. Figure 4, however, demonstrates a condition of effective penetration and optimum mixing in which the jet center line coincides with the tube axis, and these data are recorded in Table 1.

Optimum velocity ratios ($R = u_o/v$) for geometrically centered jets were determined for increasing jet Reynolds numbers Re_j as shown in Figure 5. If $Re_j > 0.9 \times 10^4$, the optimum velocity ratio R is shown to be independent of Re_j. All experimental measurements were subsequently restricted to values of Re_j greater than this value.

Figure 6 is a plot of the normalized momentum length l_m/D vs. velocity ratio R for the averaged experimental results of this study in addition to the tabulated data of other experimentalists which were judged to constitute a condition of effective mixing covering the range of $1.2 < R < 25$, $0.12 < l_m/D < 0.85$, and $Re_j \gtrsim 7.5 \times 10^3$. Superimposed on the data points is Equation (15) restricted to values of $R > 1.0$, with the indicated asymptotic limit of $l_m/D \to 0.11$ for large R.

It is apparent from Figure 6 that the averaged data of this study closely approximate that of Chilton and Genereaux (1930) taken under similar conditions. The

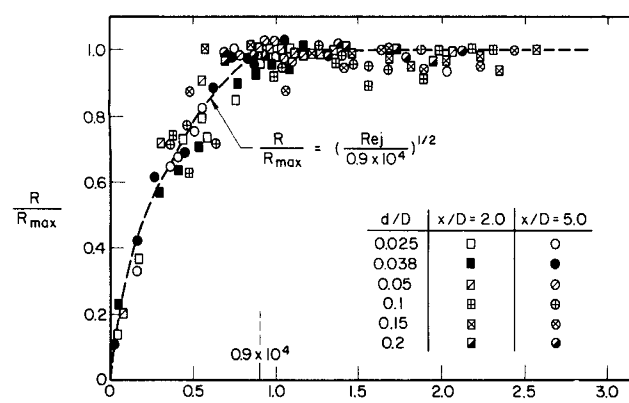

Fig. 5. Velocity ratios $R(= u_0/v)$ for geometrically centered jets as a function of jet Reynolds number Re_j.

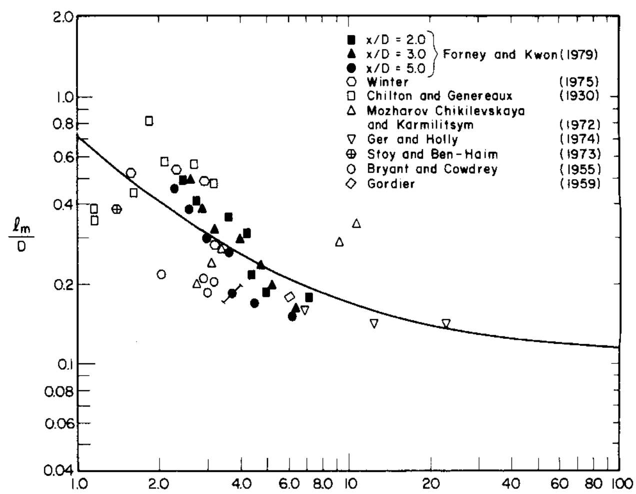

Fig. 6. Dimensionless correlation of data for conditions of optimum mixing. Solid line is Equation (15) with $\alpha = 0.11$ and $\beta = 0.6$.

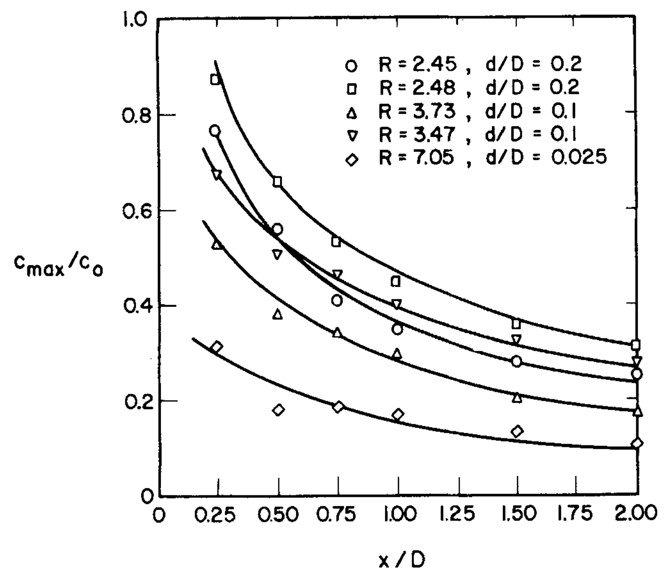

Fig. 7. Measured concentration ratios of geometrically centered jets ($x/D = 2.0$) for various values of the velocity ratio R. c_{max} represents the maximum or jet center line concentration, while c_0 is the initial jet orifice value.

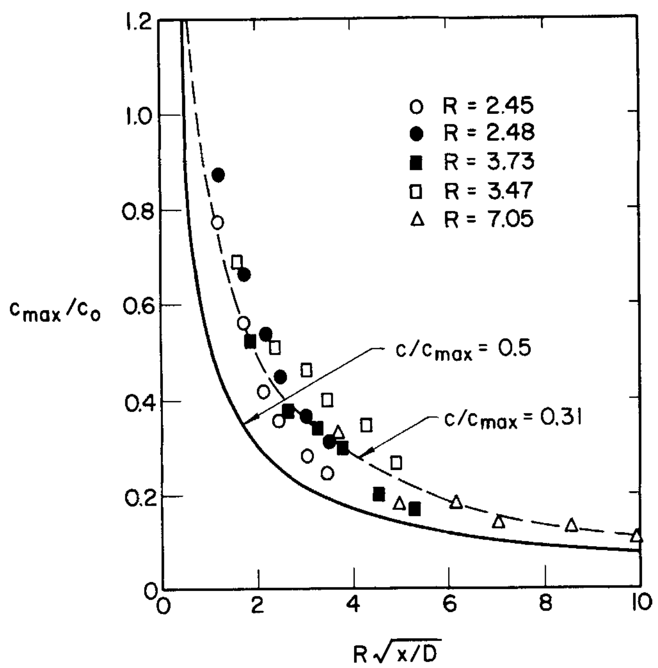

Fig. 8. Correlation of data of Figure 7 with Equation (16). The solid line represents Equation (16) assuming a Gaussian concentration profile. The dashed line is Equation (16) for the indicated ratio c/c_{max} which represents the best fit to the data, where c is the mean jet concentration for a top hat profile.

data also favorably compare with selected data of Mozharov, Chikilevskaya, and Kormilitsyn (1972) who used water as the working fluid. The latter data, as well as the selected data of Stoy and Ben-Haim (1973), Bryant and Cowdrey (1955), and Gordier (1959) using both air and water as the working fluid, were chosen from a series of recorded center-line trajectories taken by each experimentalist. The criteria used for selection were that the moving primary fluid was turbulent and that the jet and main stream center line coincided at a distance of roughly ½ to 1 duct diam from the jet orifice. In all cases, the selected trajectory appeared to level off beyond this point. The duct Reynolds number of all the data covered the range of $10^4 < Re < 5 \times 10^5$; however, no systematic variation with Re could be determined in Figure 6.

The three data points of Ger and Holley (1972) justify comment since they cover the largest values of R and exhibit the least scatter of the selected data. Their experimental technique was to measure the concentration of a salt tracer at distances up to 100 duct diam from the jet orifice at each of several normalized jet momentum lengths. The three points of Ger and Holley are those which minimize the distance required for complete mixing downstream.

In spite of the differences in experimental techniques and objectives for the data chosen, the analysis represented by Equation (15) adequately correlates the present data to within 35% and shows the correct trend over a factor of 30 variation in the velocity ratio R. Any systematic differences in the present data between measurements taken at 2, 3, and 5 duct diam ($x/D = 2.0$, 3.0, and 5.0) from the orifice are not considered to be significant, since the data coalesce with the measurements of Ger and Holley taken at $x/D \simeq 100$ and with larger velocity ratios and because of the overall scatter within the present data. The observed scatter in much of the selected data of others is due to the fact that most of it resulted from simple visual observations of the jet trajectory. Moreover, there may have been some differences in the level of ambient turbulence among the experimentalists. The data of Ger and Holley are correlated by the theory of Equation (15) to within 20%; however, the range of velocity ratios R covered by Ger and Holley was too narrow to exhibit the anticipated trend.

Measurements were also taken of the decay of the maximum or jet center line methane concentration as a function of position downstream from the jet orifice. These raw data are shown in Figure 7 and are correlated in Figure 8 with Equation (16) which has been modified to account for real concentration profiles. The solid line of Figure 8 represents the decay of the jet center line concentration for a self-similar Gaussian profile where it can be shown from a mass and momentum balance that $c_{max}/c = 2.0$ if c represents the mean concentration for a top hat profile. The dashed line of Figure 8 is Equation (16) with a ratio c_{max}/c chosen to represent the best fit to the data. Figure 8 clearly demonstrates that Equation (16) is the correct scaling law for geometrically centered jet properties, with some question remaining concerning the exact shape of the jet profiles.

ACKNOWLEDGMENT

Mr. T. C. Kwon, who conducted the experimental work, was supported by an EPA traineeship, No. EPA T 900 203.

NOTATION

b = jet radius, cm
c = mean tracer concentration, g cm^{-3}
D = tube diameter, cm
d = jet diameter, cm
l_b = buoyancy length, cm
l_D = near field length, cm
l_m = momentum length, cm
l = Prandtl eddy size, cm
R = velocity ratio, u_o/v
Re = tube Reynolds number, vD/ν
Re_j = jet Reynolds number, $u_o d/\nu$
s = axial jet coordinate, cm
t = time, s
u^* = fluid friction velocity, $\phi^{1/2}v$, cm s^{-1}

u = mean jet velocity, cm s^{-1}
v = mean tube velocity, cm s^{-1}
x = distance down tube axis from orifice, cm
z = distance along tube diameter from orifice, cm

Greek Letters

α = tangential entrainment parameter
β = normal entrainment parameter
ν = kinematic viscosity, cm^2 s^{-1}
ρ = fluid density, g cm^{-3}
θ = angle between jet and tube axes
ω = angular frequency of Prandtl eddies, s^{-1}
ϕ = friction factor, 0.04 $(Re^{-1/4})$

Subscripts

o = orifice
∞ = ambient
e = equilibrate
max = jet center line
j = jet

LITERATURE CITED

Briggs, G. A., "Plume Rise," *U.S.A.E.C. Rept. TID-25075* (1969).

Bryant, L. W., and C. F. Cowdrey, "Effects of Velocity and Temperature of Discharge on the Shape of Smoke Plumes from a Funnel or Chimney: Experiments in a Wind Tunnel," *Proc. Inst. Mech. Engrs.*, **169**, 371 (1955).

Chilton, T. H., and R. P. Genereaux, "The Mixing of Gases for Reaction," *Trans. Am. Inst. Chem. Engrs.*, **25**, 103 (1930).

Davies, J. T., *Turbulence Phenomena*, Academic Press, New York (1972).

Escudier, M. P., "Aerodynamics of a Burning Turbulent Gas Jet in a Crossflow," *Combustion Sci. Technol.*, **4**, 293 (1972).

Fay, J. A., "Buoyant Plumes and Wakes," *Ann. Rev. Fluid Mech.*, **5**, 151 (1973).

Ger, A. M., and E. R. Holley, "Turbulent Jets in Crossing Pipe Flow," *Hydraulic Engineering*, Series No. 30, Univ. Ill., Urbana (1974).

Gordier, R. L., "Studies on Fluid Jets Discharging Normally into Moving Liquid," St. Anthony Falls Hyd. Lab., University of Minnesota, Technical Paper No. 28, Series R (1959).

Hoult, D. P., J. A. Fay, and L. J. Forney, "A Theory of Plume Rise Compared with Field Observations," *J. Air Pollution Control Assoc.*, **19**, 585 (1969).

Hoult, D. P., and J. C. Weil, "Turbulent Plume in a Laminar Cross Flow," *Atmospheric Environment*, **6**, 513 (1972).

Kalinske, A. A., and C. L. Pien, "Eddy Diffusion," *Ind. Eng. Chem.*, **36**, 220 (1944).

Keffer, J. F., and W. D. Baines, "The Round Turbulent Jet in a Cross Wind," *J. Fluid Mech.*, **10**, 481 (1963).

Merzkirch, W., *Flow Visualization*, Academic Press, New York (1974).

Mozharov, N. A., A. V. Chikilevskaya, and V. I. Kormilitsyn, "Experimental Investigation of the Inflow of a Water Jet into a Turbulent Confined Water Flow at a Right Angle," *J. Thermal Eng.*, **19**, 42 (1972).

Ricou, J. P., and D. B. Spalding, "Measurements of Entrainment by Axisymmetrical Turbulent Jets," *J. Fluid Mech.*, **29**, 21 (1961).

Scorer, R. S., *Natural Aerodynamics*, Pergamon Press, Oxford, England (1958).

Slawson, P. R., and G. T. Csanady, "Turbulent Jets in Crossing Pipe Flow," *J. Fluid Mech.*, **47**, 311 (1967).

Stoy, R. L., and Y. Ben-Haim, "Turbulent Jets in a Confined Crossflow," *ASME Paper No. 73-FE-15* (1973).

Winter, D. D., "Mixing of a Turbulent Jet in a Turbulent Cross Flow," M.S. thesis, Univ. Ill., Urbana (1975).

APPENDIX

Effect of Buoyancy

The derivation in the text leading to the correlation represented in Figure 6 assumes the jet is not buoyant relative to the ambient fluid or is at most weakly buoyant, that is, $\rho_o \simeq \rho_\infty$. To generalize the results of Figure 6 to include the effects of buoyancy for a jet with both an initial momentum and buoyancy flux at the orifice, one can distinguish between the effects of large density disparities on the entrainment rate in the momentum dominated region near the orifice from these buoyant effects further downstream where the flow is accelerated entirely by buoyant forces. While the extent of the momentum dominated region for weakly buoyant plumes has been shown by Hoult et al. (1969) to be $x < x_c$ where

$$x_c = \left(\frac{2\beta^2}{3}\right)^2 \left(\frac{1}{\alpha + \beta/R}\right)^3 \frac{l_m{}^3}{l_b{}^2} \tag{A1}$$

and

$$l_b = \frac{u_o b_o{}^2 g}{v^3} \left| \frac{\rho_\infty - \rho_o}{\rho_\infty} \right|$$

where l_b is the buoyancy length scale, the effect of large density differences on jets near the orifice when $x < x_c$ may be accounted for as suggested by Escudier (1972). Escudier included the results of Ricou and Spalding (1961) who measured the entrainment rates of buoyant turbulent jets in the analysis of Hoult et al. Ricou and Spalding found that one could correlate their data by using an equivalent entrainment parameter of magnitude $\alpha(\rho/\rho_\infty)^{1/2}$ in place of α. By scaling the entrainment parameters α and β in this manner, Escudier derived the near field solution in the momentum dominated region which was identical in form to Equation (12) with one exception. Escudier found that $l_m = (du_o/v)(\rho_o/\rho_\infty)^{1/2}$ in his results. Thus, in Equations (15) and (A1) and Figure 6, the appropriate dimensionless groups are

$$\frac{l_m}{D} = \left(\frac{du_o}{Dv}\right)\left(\frac{\rho_o}{\rho_\infty}\right)^{1/2} \tag{A2}$$

and

$$R = \left(\frac{u_o}{v}\right) \tag{A3}$$

for $\rho_o/\rho_\infty \neq 1$.

Therefore, the proposed scaling law for effective mixing of Equation (15) is valid for buoyant jets with one restriction. This restriction is derived from the fact that the analysis leading to Equation (15) assumes the flow is dominated by momentum for $x < l_D$, which implies that $x_c > l_D$ from Equation (A1) above. Normalizing Equation (A1) with respect to the duct diameter D, using Equations (15), (A1), and (A2) and letting $x_c > l_D$ where $l_D/D = 1/2$, one finds

$$\frac{l_b}{D} < \left(\frac{2^{3/2}\beta^2}{3}\right) \tag{A4}$$

for the neglect of buoyancy in the near field and the analysis leading to Equations (15) and (A2) to hold. This restriction can be shown to mean that to within a constant of order one the densimetric Froude number must be greater than the velocity ratio or $F_r > R$, where

$$F_r = u_o \Bigg/ \left(g b_o \left| \frac{\rho_\infty - \rho_o}{\rho_\infty} \right| \right)^{1/2}$$

for the neglect of buoyancy in Equation (15).

Since the majority of the data points used in the correlation of Figure 6 were the results of experiments using nonbuoyant jets and no systematic variation could be found within the scatter of the data for that data taken under buoyant conditions, the correlation suggested by Equations (A2) and (A3) was not used. However, additional experiments should be conducted to show these effects.

Jet Travel Distance

An important assumption in the development of Equation (15) is that a parcel of fluid within the jet travels a distance l_D down the tube axis from the orifice in time ω^{-1}. This would be the case if the jet immediately equilibrated with the ambient fluid at the orifice. However, a fluid parcel within the jet travels for a short time in a direction perpendicular to the tube flow.

Here, the analysis is restricted to a region near the orifice where $s \simeq z$, or to the lowest order

$$\frac{dz}{dt} = u_o \tag{A5}$$

and

$$\frac{dz}{dt} = \frac{1}{2}\left(\frac{l_m}{x}\right)^{1/2}\left(\frac{1/2}{\alpha + \beta/R}\right)^{1/2}\frac{dx}{dt} \tag{A6}$$

from Equation (16) where x, z refer to the coordinates of a fluid parcel within the jet. Letting $K = 2^{1/2}(\alpha + \beta/R)^{1/2}$ where $K = 0(1)$ for all R and combining Equations (A5) and (A6), one has

$$\frac{1}{v}\frac{dx}{dt} = 2\,KR\left(\frac{x}{l_m}\right)^{1/2} \tag{A7}$$

From Equation (A7) it is seen that a parcel of fluid within the jet will equilibrate with the ambient fluid when $1/v\ dx/dt \to 1$, or at

$$x_e = \frac{l_m}{4\ K^2R^2} \quad \text{for} \quad R > 1.0 \tag{A8}$$

This occurs in a travel time t_e, where

$$t_e = \frac{1}{v}\left(\frac{l_m^{1/2}}{2\,KR}\right)\int_0^{x_e}\frac{dx}{x^{1/2}} \tag{A9}$$

by the integration of Equation (A7). Thus the equilibration time is

$$t_e = \frac{1}{2\,vK^2}\left(\frac{l_m}{R^2}\right) \quad \text{for} \quad R > 1.0 \tag{A10}$$

or the total travel distance of the fluid parcel at the end of the near field when $t = \omega^{-1}$ is

$$x = x_e + v(\omega^{-1} - t_e) \tag{A11}$$

where $v/\omega = l_D$. Substitution of Equations (A8) and (A10) into Equation (A11) gives, with some rearrangement

$$\frac{x}{l_D} = 1 - \left(\frac{1}{4\,K^2}\right)\left(\frac{l_m}{l_D}\right)\left(\frac{1}{R^2}\right) \quad \text{at} \quad t = \omega^{-1} \quad \text{and} \quad R > 1.0 \tag{A12}$$

where $1 < 2K < 2.4$ and $l_D/l_m = 0(1)$ for $1 < R < \infty$. Thus, the assumption that jet fluid parcels near the orifice travel a distance equal to that of the ambient fluid for times on the order of ω^{-1} appears to be a reasonable one.

Manuscript received October 23, 1978; revision received March 2, and accepted March 26, 1979.

Surface Ablation in the Impingement Region of a Liquid Jet

MICHAEL J. SWEDISH
MICHAEL EPSTEIN
JOHN H. LINEHAN
GEORGE A. LAMBERT
GEORGE M. HAUSER
and
LARRY J. STACHYRA

Argonne National Laboratory
9700 South Cass Avenue
Argonne, Illinois 60439

A theoretical and experimental investigation of a water jet impinging on a melting solid surface has been carried out. Ice, octane, *p*-xylene, and olive oil served as the meltable solid materials, comprising a Prandtl number range of 5 to 2 800. An available laminar stagnation flow model was utilized to describe melting heat transfer in the jet impingement region. Melting rate measurements were found to agree quite well with the values predicted with this model.

SCOPE

Fluid jets impinging on surfaces result in high rates of heat transfer as compared with most other forced convection flow geometries. This fact has led to the recent application of hot liquid or gaseous jets to drill through solid material (Mellor, 1974). An important feature of the flow in this application is the insulating effect of the thin layer of melt which forms between the impinging jet and the melting solid. Melting in the impingement region of a fluid jet is also important in other practical situations; for example, the aerospace industry relies on meltable materials to relieve aerodynamic heating in the stagnation region of spacecraft requiring atmospheric entry; the integrity of protective steel barriers when subjected to jets of molten reactor material is an important safety question in current design of in-pile experiments that attempt to simulate postulated core disruptive accidents for the fast breeder reactor; and melting can be exploited to delineate heat transfer rates for liquid jets impinging on nonmelting surfaces.

While many studies have been reported on the heat and mass transfer characteristics of impinging fluid jets, the attention of researchers has overwhelmingly remained focused on gas jets. Relatively little work has been reported on the heat transfer between a liquid jet and the surface on which it impinges. Sitharamayya and Subba Raju (1969) performed the only experimental study of heat transfer between a submerged liquid (water) jet and a flat solid surface held normal to the flow. Yen and Zehnder (1973) studied ablation of ice by a liquid (water)

Correspondence concerning this paper should be addressed to Michael Epstein. Michael J. Swedish is with Wisconsin Electric Power Company, Milwaukee, Wisconsin. John H. Linehan is with Marquette University, Milwaukee, Wisconsin.